REVIEW ARTICLE
PUBLISHED ONLINE: 21 JUNE 2016 | DOI: 10.1038/NCHEM.2547

nature chemistry

Dynamic molecular crystals with switchable physical properties

Osamu Sato

The development of molecular materials whose physical properties can be controlled by external stimuli — such as light, electric field, temperature, and pressure — has recently attracted much attention owing to their potential applications in molecular devices. There are a number of ways to alter the physical properties of crystalline materials. These include the modulation of the spin and redox states of the crystal's components, or the incorporation within the crystalline lattice of tunable molecules that exhibit stimuli-induced changes in their molecular structure. A switching behaviour can also be induced by changing the molecular orientation of the crystal's components, even in cases where the overall molecular structure is not affected. Controlling intermolecular interactions within a molecular material is also an effective tool to modulate its physical properties. This Review discusses recent advances in the development of such stimuli-responsive, switchable crystalline compounds — referred to here as dynamic molecular crystals — and suggests how different approaches can serve to prepare functional materials.

An important challenge in molecular materials science is the design of functional compounds whose physical properties can be controlled by external stimuli — making them promising for a range of practical applications[1–13]. Numerous molecular materials exhibiting various switching effects in their electronic, magnetic, optical and mechanical properties — controlled through a variety of phenomena — have recently been reported, and are herein called dynamic molecular crystals (Fig. 1). Here, some representative examples are discussed, under the categories of spin transition[1,2], charge transfer[3–5], proton transfer[6,7], change in molecular structure[8–11], and change in molecular orientation (Fig. 2)[11,12]. The 'Charge transfer' section is further divided into two parts: charge transfer and charge-transfer-coupled spin transition. These categories are used here for clarity, but they are not completely separate from each other. Polyatomic entities in which atoms are linked through covalent or coordination bonds are defined as molecules in the present Review, and phenomena resulting from the rearrangement of other chemical interactions, such as hydrogen bonds, are included in the section 'Change in molecular orientation', rather than 'Change in molecular structure'. Proton transfer has been given its own section, although it can also be seen as a type of molecular structural change. Similarly, the spin-transition and charge-transfer processes, discussed in separate sections, inevitably induce molecular structural changes. Furthermore, changes in a molecular structure are also accompanied by a modification of the electron distribution in the molecule.

Too many dynamic molecular crystals have been reported for them to all be included in this Review. Therefore, only representative examples are introduced and discussed in the text, with a focus on systems with atypical dynamic properties. For example, spin transitions have mostly attracted attention in terms of change in magnetic properties, but they have also been used to switch conducting and mechanical properties of compounds. Charge- and proton-transfer processes, essential in biological systems, have recently been used in synthetic systems to control optical, ferroelectric, and conducting properties. Unusual photomechanical properties have also been engineered using several photochromic molecules that more commonly serve to control optical properties. Change in the molecular orientation within a material, including molecular rotation and displacement, have resulted in polarization switching and a change in mechanical properties. These unusual and intriguing phenomena are the main topic of this Review.

To obtain dynamic molecular crystals, the design of appropriate electronic characteristics through the ligand field and redox potential of the components is essential. It is also important to control the molecular arrangement within a crystal because it governs its dynamic properties. For example, processes such as molecular dimerization, intermolecular charge transfer and intermolecular proton transfer only occur when the participating molecules are suitably assembled within a crystal. Furthermore, intermolecular interactions also play a key role in a material's response to external stimuli. The introduction of, for example, π-π interactions, coordination bonds, and hydrogen bonds can make dynamic behaviours cooperative, allowing the observation of a bistable character in the switching process. Note that bistability refers to the ability of a system to take two different stable states in a certain range of an external perturbation (Fig. 1b) — for example spin crossover between high-spin (HS) and low-spin (LS) states, charge transfer, and charge-transfer-coupled spin transitions that occur over a temperature range. In the absence of these intermolecular interactions in a molecular crystal, thermally induced transitions occur gradually. In the presence of strong intermolecular interactions however thermal transitions often becomes abrupt, sometimes with hysteresis (Fig. 1b)[14], because of the occurrence of a cooperative transition in the crystal. The induction of such a phase transition in a bistable system is a useful method to achieve an efficient switching behaviour, because the system exhibits large responses to subtle external stimuli[15].

Dynamic molecular crystals can also be designed by combining two or more components. In particular, molecules that undergo a reversible switch in the crystalline state can be combined with another functional building block, and used as switching units to control the overall properties of the resulting multi-component material. For example, combining spin-crossover complexes (working as 'switching units') with molecular conductors can give materials able to undergo conductivity switching. Two or more molecules can be combined, for example, using electrostatic interactions in ionic crystals or coordination bonds in metal complexes wherein tunable molecules are used as ligands.

By discussing phenomena ranging from spin transitions to molecular orientation changes, this Review aims to show how the

Institute for Materials Chemistry and Engineering, Kyushu University, 744 Motooka Nishi-ku, Fukuoka, 819-0395, Japan. e-mail: sato@cm.kyushu-u.ac.jp

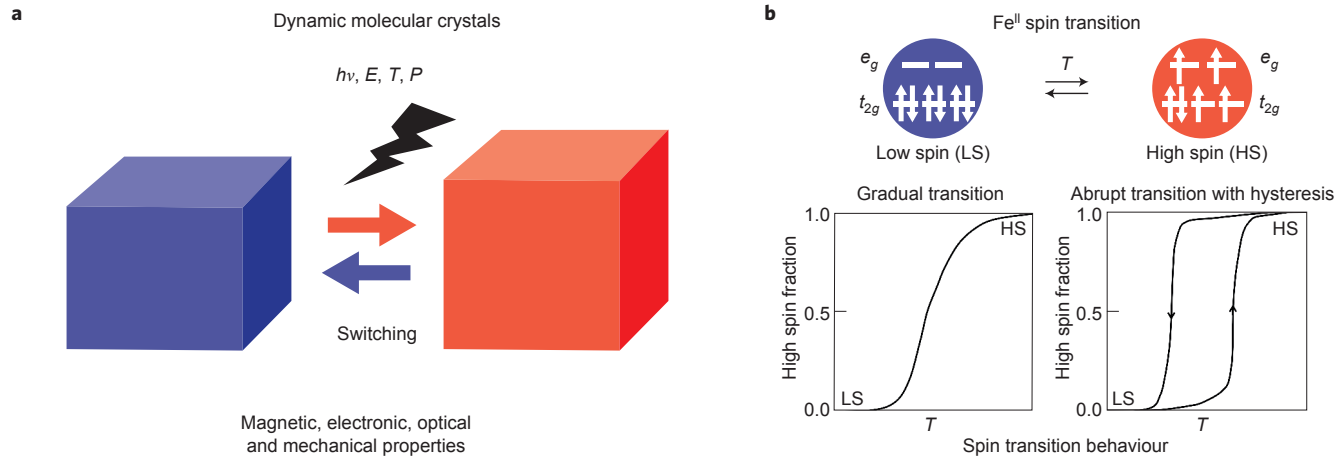

Figure 1 | Dynamic molecular crystals wherein physical properties are switched by external stimuli such as light, electric field, temperature and pressure. a, Schematic of molecular crystalline materials that exhibit a dynamic change in physical properties in response to external stimuli such as light irradiation (*hν*), electric field (*E*), temperature (*T*), and pressure (*P*). **b**, Spin transition behaviour in crystalline Fe^{II} spin transition compounds, which are typical examples of dynamic molecular crystals. Top, spin transition behaviour in the 3*d* orbitals. When intermolecular interactions are weak, gradual spin transition occurs, as shown in the graph on the left. On the other hand, when intermolecular interactions are strong, the thermal transition becomes abrupt (transition occurs in a narrow temperature range). In some cases, the abrupt transition also involves hysteresis, as shown in the graph on the right wherein the transition temperatures of the cooling and heating modes are different[14]. In the temperature range within the hysteresis loop, the spin transition compound can have two different states (HS and LS); this property is known as bistability.

precise control of electron, proton, and molecular movement within crystals through the application of external stimuli can lead to considerable changes in the crystals' properties. It also aims to show that the approach taken in a given field may be applicable to other ones. For example, photoinduced molecular structural change, used to switch optical properties in the field of photochromism, can also be used to control magnetic properties. Proton transfer and molecular displacement mechanisms, used to switch the polarization of materials in the field of ferroelectrics, can also be used to control characteristics such as conductivity.

Spin transition

Octahedral metal complexes that are based on a transition metal with d^4–d^7 configurations can adopt either a HS or LS state. The state adopted is determined by the complex's ligand field strength, however in some cases — when the mean pairing energy required to accommodate two electrons in one orbital is between the ligand field splitting of the HS and LS states — it may be possible to induce a crossover between the HS and the LS states by a temperature change[1,2,16]. More specifically, when the enthalpy of the entropically favourable HS state is only slightly higher than that of the LS state, entropy (S^{etp}) driven spin crossover from LS of the low-temperature (LT) phase to HS of the high-temperature (HT) phase is observed. The entropy gain in the HS state arises from both electronic (ΔS^{etp}_{el}) and vibrational (ΔS^{etp}_{vib}) contributions, where ΔS^{etp}_{el} is derived mainly from spin degeneracy, because orbital degeneracy is generally removed since the structure around the metal centre in typical spin-crossover compounds normally deviates from an ideal symmetrical structure[17]. Spin-crossover phenomena have been observed in molecules both in crystalline and solution states.

The dependence of the spin transition behaviour on temperature is shown in Figure 1b. For a molecular crystal without strong intermolecular interactions, the thermally induced spin transition is gradual (Fig. 1b, left). In the presence of strong intermolecular interactions however it becomes abrupt, and sometimes exhibits hysteresis in temperature-dependent magnetization plots (Fig. 1b, right)[1]. Within the hysteresis loop, a compound can adopt two electronic states — this bistability is essential for practical applications. The spin-crossover behaviour of a complex is normally accompanied by a change in its optical and dielectric properties[18–20], for example a change in colour — this has been applied to prepare display devices[18].

In some cases, a spin transition can be induced by light irradiation rather than a temperature change. This is the case in Fe^{II} and Fe^{III} spin-crossover complexes, and is known as the light-induced excited spin state trapping (LIESST) effect[16,21,22]. Fe^{II} moieties exhibiting the LIESST effect (photoinduced transformation from LS to HS) were incorporated into a CN-bridged coordination polymer with the structure Nb^{IV}–CN–Fe^{II}–NC–Nb^{IV}. In this system, photoinduced ferrimagnetic ordering was observed as a result of the photoinduced transformation from Fe^{II}_{LS} to Fe^{II}_{HS}, which switches the magnetic interaction between the metal centres[23]. Furthermore, spin transition systems can respond to additional stimuli: the application of external pressure can also induce a conversion from the HS to the LS state[24,25].

Recently, single-molecule magnet (SMM) behaviour has been observed that arose through the LIESST process. Molecules that exhibit slow reversal of magnetization, even a hysteresis loop below a certain temperature due to the energy barriers arising from pure molecular origin (that is, large spin ground-states and large zero field splittings) are called SMMs (ref. 26) — the archetypal SMM being $[Mn_{12}O_{12}(CH_3COO)_{16}(H_2O)_4]\cdot 2CH_3COOH\cdot 4H_2O$, often referred to as {Mn12}. Engineering SMMs so that they are responsive to external stimuli would make them very useful for applications such as in memory devices[27–29]. Several phototunable multinuclear SMM compounds have been reported, with charge transfer and photoisomerization for photoswitching mechanisms[28,29]. Recently, mononuclear Fe^{II} complexes have also been reported whose HS metastable states, induced via the LIESST process, exhibit SMM behaviour after irradiation[30,31]. In particular, the reversible switching of SMM properties was observed in the Fe^{II} complex $[Fe(1\text{-propyltetrazole})_6](BF_4)_2$ (Fig. 2a), through irradiation at 505 nm and 850 nm light, which induce LIESST and reverse LIESST (photoinduced transformation from HS to LS), respectively[30]. When these Fe^{II} moieties were incorporated in a CN-bridged one-dimensional (1D) structure, single-chain magnetic (SCM) behaviour was observed through the LIESST process[32] — which is different from the magnetic behaviour in typical bulk magnets. The preparation of such phototunable SMMs and SCMs is essential for the development of high-density photorecording devices.

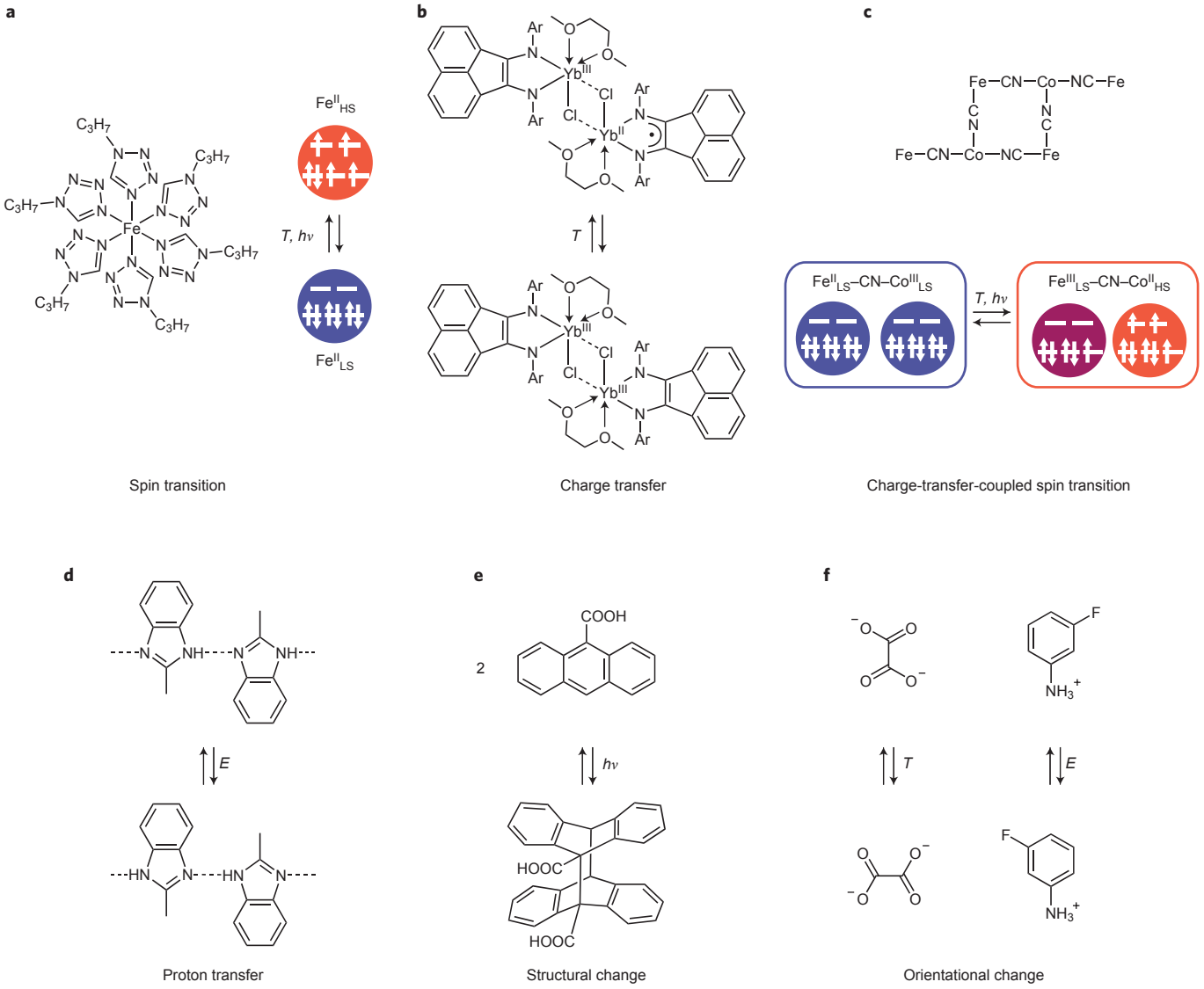

Figure 2 | Examples of systems in which the physical properties of molecular crystalline materials are altered by manipulating spin, electron transfer, proton transfer, molecular structure and orientation. a, Spin transition in an Fe^{II} complex $[Fe^{II}(1\text{-propyltetrazole})_6]^{2+}$ (refs 16,21). **b**, Charge transfer between Yb and a ligand in a dinuclear Yb complex [{(dpp-bian)Yb(μ-Cl)(1,2-dimethoxyethane)}$_2$] (Ar = 2,6-diisopropylphenyl)[3,64]. See 'Charge transfer' section and Fig. 4b for further details. **c**, Charge-transfer-coupled spin transition in a cyanide-bridged hexanuclear Fe_4Co_2 complex[4,29]. **d**, Proton transfer between 2-methylbenzimidazole molecules under an external electric field[94]. **e**, Structural change via photoinduced [4 + 4] cyclodimerization reaction of two 9-anthracenecarboxylic acid molecules[106]. **f**, Orientation change of an oxalate anion (left) and an *m*-fluoroanilinium cation (*m*-FAni$^+$, right), which exhibit 90° rotation and 180° flip-flop motion, respectively, within the crystalline lattices of $[Ni^{II}(en)_3](ox)$ (en = ethylenediamine and ox = oxalate anion) and (*m*-FAni$^+$)(crown-ether). See text and Fig. 8 for further details[126,129].

A spin-crossover behaviour in a complex is normally accompanied by structural changes. The molecular volume of a HS state is larger than that of a LS state because the e_g orbitals — which host more electrons when a metal is in its HS state than its LS state — exhibit anti-bonding character. This change in structure at a molecular level induces crystal deformation at the spin transition temperature, and can serve to promote a mechanical effect. This was demonstrated in a bilayer film composed of a spin-crossover layer and an aluminium layer. The spin-crossover phenomenon induced significant bending of the film around the transition temperature, in a similar manner to the bending of bimetallic strips under a temperature change owing to the difference in thermal expansion of the two metals[33].

Changes in molecular structure at the spin-crossover temperature have also been used to modulate the conductivity in materials comprising both a spin-crossover complex and a conducting molecule[34–36]. In the $[Fe^{III}(qnal)_2][Pd(dmit)_2]_5$·acetone salts (Hqnal = *N*-(8-quinolyl)-2-hydroxy-1-naphthaldimine, $dmit^{2-}$ = 1,3-dithiole-2-thione-4,5-dithiolato), the $Pd(dmit)_2$ molecules form a two-dimensional conducting layer. The change in volume at the molecular level between the HS and LS states in $[Fe^{III}(qnal)_2]^+$ induces uniaxial strain in the $[Fe^{III}(qnal)_2][Pd(dmit)_2]_5$·acetone salt, which in turn affects its conductivity, resulting in the appearance of a conductivity anomaly at the spin transition temperature of the Fe^{III} complex (around 200 K)[35]. Another example of a spin-crossover-based conductor is $[Fe^{II}(tpma)(xbim)](ClO_4)(TCNQ)_{1.5}$·DMF (tpma = tris(2-pyridylmethyl)amine, xbim = 1,1′-(α,α′-*o*-xylyl)-2,2′-bisimidazole, TCNQ = 7,7′,8,8′-tetracyanoquinodimethane)[36]. The change in the activation energy (E_a) of the complex occurs at approximately 100–125 K (which corresponds to the area between 8×10^{-3} and 10×10^{-3} K^{-1} on the $1/T$ plot on the right of Fig. 3a). This temperature corresponds to the one at which the spin transition

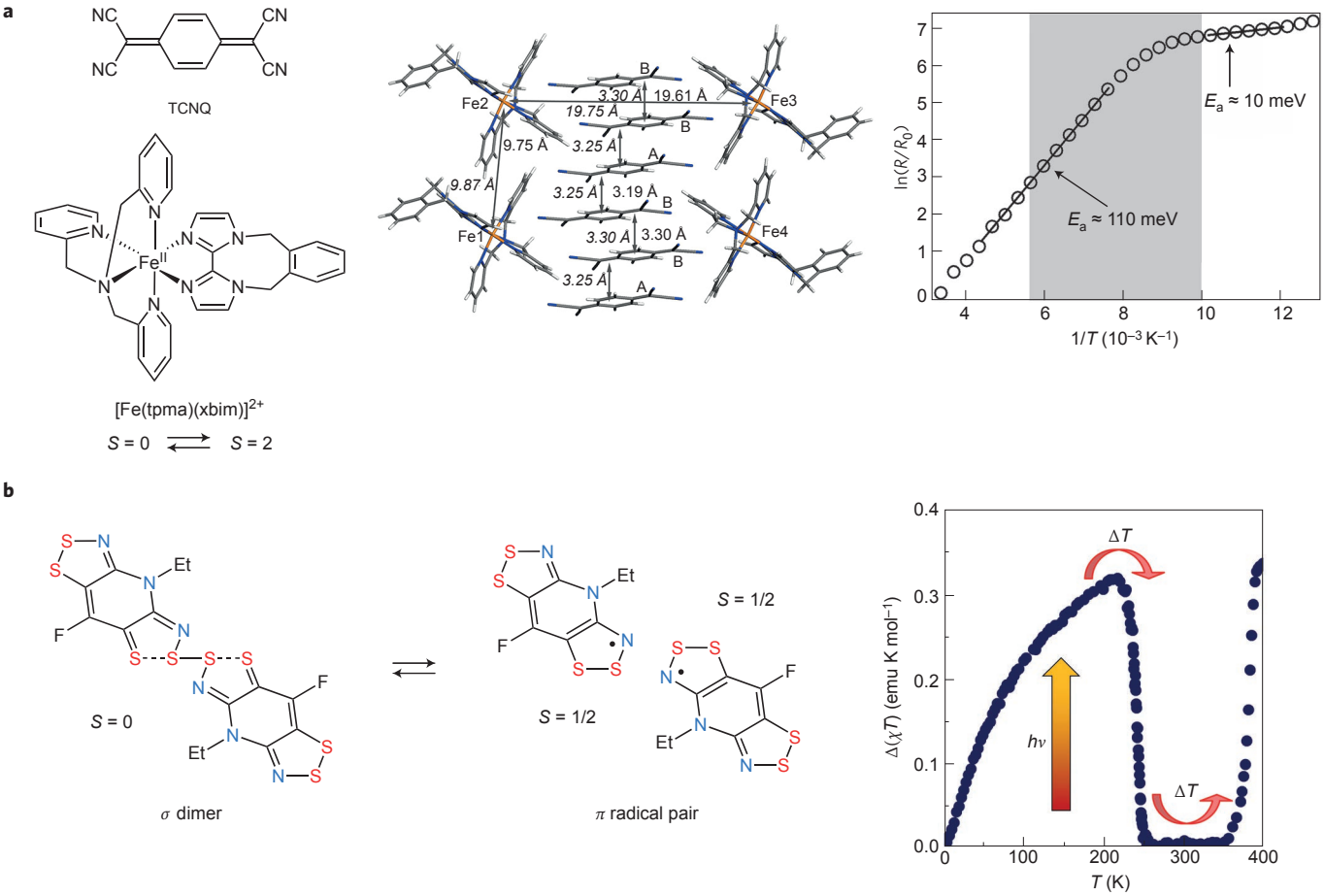

Figure 3 | Control of physical properties through the induction of spin transition. a, Left, molecular structure of TCNQ and $[Fe(tpma)(xbim)]^{2+}$. Middle, single crystal structure of $[Fe(tpma)(xbim)](ClO_4)(TCNQ)_{1.5}$·DMF with interatomic distances at 230 K (italic font) and 100 K (regular font); Orange (Fe), blue (N), grey (C) and white (O). Right, dependence of the relative resistance on the inverse temperature. The change in the activation energy (E_a) takes place between 100 and 125 K, that is, between 10×10^{-3} and 8×10^{-3} K^{-1} (right side of shaded area) in the $1/T$ plot, which coincides with the completion of the spin transition from the HS to LS state. This means that the spin state of the Fe^{II} complex influences the conductivity of the salt[36]. **b**, Left, solid-state conversion between a π-radical pair and a σ-dimer of a bisdithiazolyl radical[43]. Right, change in χT on warming after irradiation ($\lambda = 650$ nm) at 10 K. The abrupt decrease in χT around 242 K is due to relaxation from the photoinduced metastable π-radical pair to the σ dimer. The abrupt increase in χT around 380 K on further warming is attributable to the thermally induced transformation from the σ dimer to the π-radical pair[43]. Figures reproduced from ref. 36, Wiley (**a,** middle and right); and ref. 43, American Chemical Society (**b**, right).

from HS to LS is completed, showing the presence of synergy between the spin transition and conductivity in the compound.

Many organic radicals also exhibit a reversible conversion between monomers that exhibit S (spin quantum number) = 1/2 and dimers with $S = 0$, which is accompanied by a change in the system's magnetic properties. This transformation, which involves a change in the spin state of the organic species, is often called spin transition (or spin crossover), although its mechanism is very different from the spin transition of coordination compounds discussed above[37–46]. Several of these compounds also exhibit thermal hysteresis[39]. Photomagnetic properties were observed in a bisdithiazolyl radical[43], which exhibits dimer-to-radical interconversion at approximately 380 K with a narrow hysteresis loop of 5 K (ref. 42). When the σ dimer of the bisdithiazolyl radical is excited with a light wavelength of 650 nm at 10 K, a substantial increase in magnetization was observed as the σ dimer ($S = 0$) converted to a pair of π radicals (each with $S = 1/2$) on breakage of the central σ bond (Fig. 3b)[43]. The relaxation temperature from the meta-stable π radicals back to the σ dimer is approximately 242 K. This temperature of 242 K is higher than those of any Fe^{II} or Fe^{III} LIESST complexes, which is an important advancement toward practical applications at room temperature. Furthermore, a two-step spin transition was recently reported in a linear array of the organic compound 3′-methylbiphenyl-3,5-diyl bis(tert-butylnitroxide) ($S = 1$) (ref. 46). This system is somewhat unusual in that the spin state changes from $S = 0$ to $S = 1$ through $S = 1/2$, rather than the typical change of spin in organic compounds between $S = 0$ and $S = 1/2$.

In the future, spin-crossover complexes may be more widely used as switching units to modulate various materials properties by combining them with other functional molecules. Organic radicals provide new types of spin-crossover behaviour, and the recent achievement of a high relaxation temperature (242 K) (ref. 43), mentioned above (Fig. 3b), suggests that they may have potential for future photomagnetic applications.

Charge transfer

Dynamic change in the physical properties of molecular compounds can also be induced by modulating redox states through charge transfer. Several organic charge-transfer complexes — comprising an electron-donor (D) and an electron-acceptor (A) — are known to exhibit a thermal neutral–ionic transition via charge transfer between D and A (refs 47,48). Such a neutral–ionic transition is observed when the difference between the ionization potential of D (I_D) and the electron affinity of A is close to the electrostatic

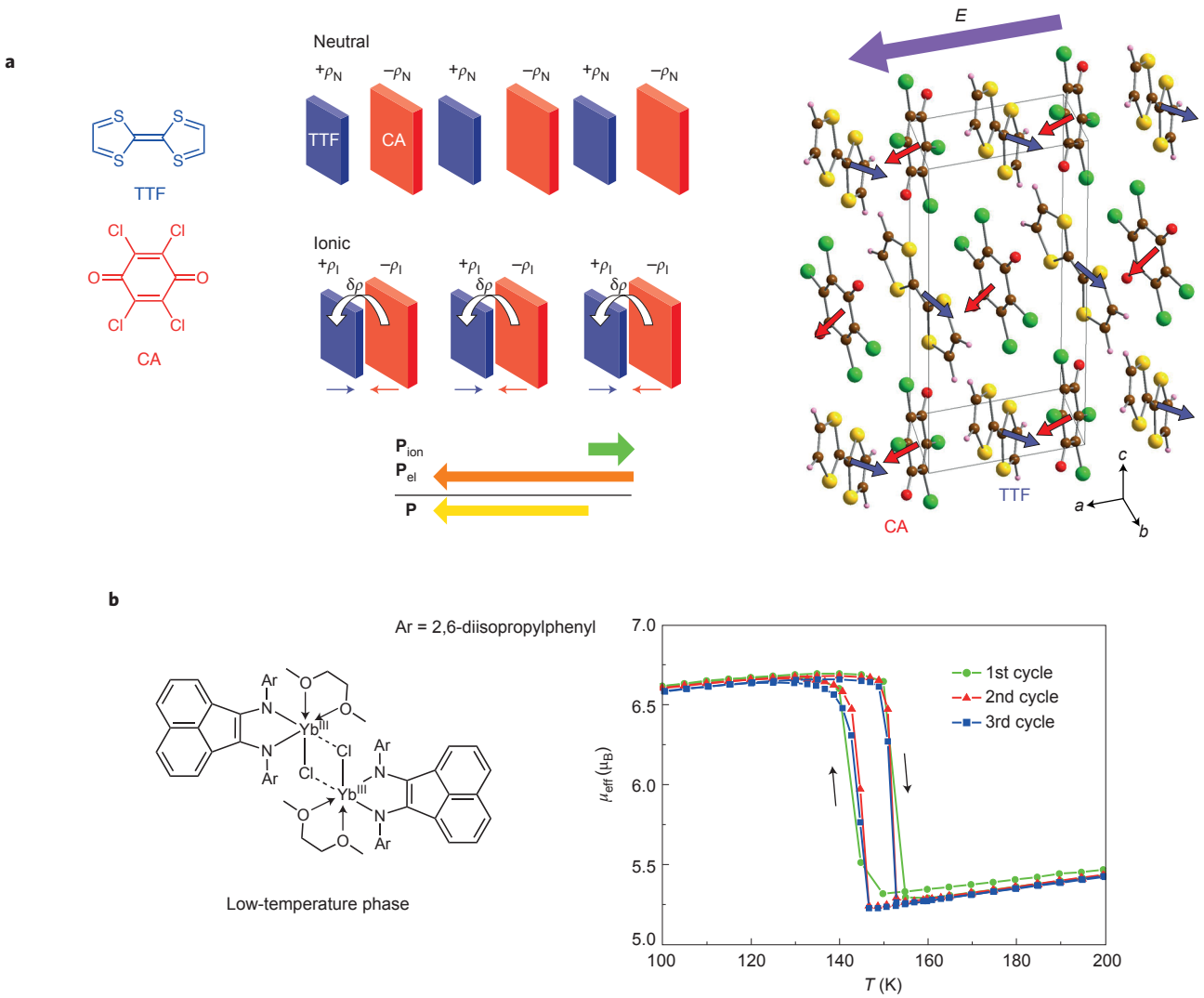

Figure 4 | Control of physical properties through the induction of charge transfer. a, Left, molecular structures of TTF and CA. Middle, schematic of neutral and ionic phases of the TTF–CA. The displacement directions of TTF and CA are depicted by blue and red arrows, respectively; ρ_N = degree of charge transfer in the neutral phase (ρ_N ~ 0.3), ρ_I = degree of charge transfer in the ionic phase (ρ_I ~ 0.6), $\mathbf{P}_{ion}$ = polarization in the ionic phase due to molecular displacements, $\mathbf{P}_{el}$ = polarization in the ionic phase due to fractional charge transfer ($\delta\rho$), and $\mathbf{P} = \mathbf{P}_{ion} + \mathbf{P}_{el}$ = net polarization. The direction of **P** is opposite to that of $\mathbf{P}_{ion}$ (refs 51,53). Right, crystal structure of TTF–CA and molecular displacement directions under application of electric field; positively charged TTF and negatively charged CA are displaced against the electric field[51,53]. Yellow (S), brown (C), red (O), green (Cl), orange (H). **b**, Left, molecular structure of [{(dpp-bian)Yb(μ-Cl)(1,2-dimethoxyethane)}$_2$] at low temperature phase. Right, plot of μ_{eff} versus T for a single crystal of the dinuclear Yb complex[64]. Figures reproduced from ref. 51, APS (**a**, right); and ref. 64, Wiley (**b**, right).

energy, called Madelung energy (M). The driving force of the transition is an increase of the Madelung energy induced by thermal contraction; the neutral and ionic states correspond to the HT and LT phases, respectively. Such neutral–ionic transitions can also be induced by pressure[49].

A typical compound exhibiting neutral–ionic transition is the charge-transfer complex between tetrathiafulvalene (TTF) as the electron donor and *p*-chloranil (CA) as the electron acceptor[47,50], for which the neutral–ionic transition temperature is approximately 81 K. Below that, TTF–CA exhibits ferroelectric properties — that is, a spontaneous electric polarization that can be reversed under an external electric field.

Typically, the displacement of cations and anions from their symmetric positions can induce a polar structure in crystals — this is an important mechanism of ferroelectric phase transitions. For most donor–acceptor compounds that undergo such a ferroelectric polarization, the ferroelectric properties are accounted for by the components' ionic displacement (as static charges) under an electric field. In the case of the TTF–CA compound however, neither the direction nor the magnitude of the components' displacement correspond to those expected with the static-point charge model. Recently, this has been explained by the fact that its ferroelectric properties are governed by intermolecular charge transfer instead[51–53], as shown in Fig. 4a. This type of electronic ferroelectricity has recently attracted considerable attention, and the generation of polarization originating from charge disproportionation has been identified in several compounds[54–56], including α-(BEDT–TTF)$_2$I$_3$ (BEDT–TTF = bis(ethylenedithio)tetrathiafulvalene)[56].

Charge transfer has also been observed between two different metal centres in coordination compounds. One such example is a bimetallic pentadecanuclear cluster, $\{Fe_9[W(CN)_8]_6(MeOH)_{24}\}\cdot x$MeOH. Thermal charge transfer occurs within the clusters, accompanied by a change in both the oxidation states and the spin quantum number of Fe and W: the LT phase consists of $W^{IV}_{(S=0)}$–CN–$Fe^{III}_{HS(S=5/2)}$ and the HT phase of $W^{V}_{(S=1/2)}$–CN–$Fe^{II}_{HS(S=2)}$ (ref. 57). This charge-transfer process is reminiscent of that of the iron compound

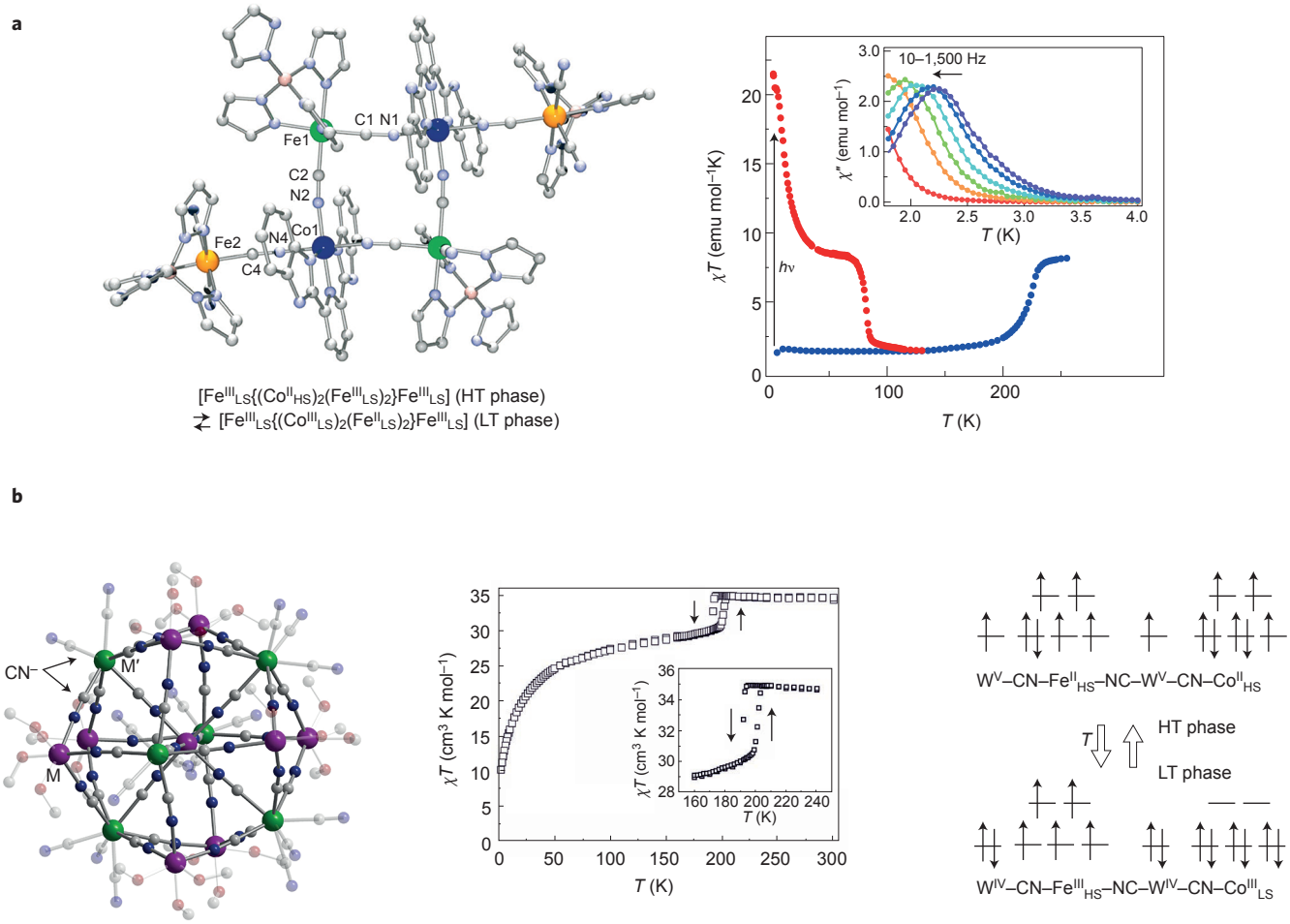

Figure 5 | Control of physical properties through the induction of charge-transfer-coupled spin transition. a, Left, molecular structure of $[Co_2Fe_4(bimpy)_2(CN)_6(\mu\text{-}CN)_6(pztp)_4]\cdot 2(1\text{-}PrOH)\cdot 4H_2O$. Right, plots of χT versus T before (blue) and after (red) light irradiation. Inset: plots of χ'' versus T after light irradiation with H_{ac} = 3 Oe oscillating at 10–1,500 Hz and H_{ext} = 500 Oe; χ'' = alternating current magnetic susceptibility (out-of-phase signal), H_{ac} = alternating current magnetic field, and H_{ext} = external direct current magnetic field[29]. **b**, Left, molecular structure of the $M^{II}{}_9M'^{V}{}_6$ clusters; large purple spheres (3*d* M ions), large green spheres (4*d* or 5*d* M′ ions), small grey spheres (C), small blue spheres (N) and small red spheres (O). Middle, plot of χT versus T. Right, thermal change in redox state in $\{Co^{II}{}_3Fe^{II}{}_6[W^{V}(CN)_8]_6(MeOH)_{24}\}\cdot x$MeOH (ref. 80). Figure reproduced from ref. 29, Wiley (**a**); and ref. 80, Wiley (**b**, middle).

$(n\text{-}C_3H_7)_4N[Fe^{II}Fe^{III}(dto)_3]$ (dto = 1,2-dithiooxalate)[58,59], in which the difference in the spin entropy between the LT phase with $Fe^{II}{}_{LS(S=0)}$-dto-$Fe^{III}{}_{HS(S=5/2)}$ and HT phase with $Fe^{III}{}_{LS(S=1/2)}$-dto-$Fe^{II}{}_{HS(S=2)}$ is a major factor in driving the phase transition. The magnetic properties of the WFe cluster show a 'reverse' thermal hysteresis loop at the charge-transfer phase transition temperature, in which the χT (χ = molar magnetic susceptibility) value of the HT phase is smaller than that of the LT phase. This is in contrast to the spin transition and charge-transfer-coupled spin transition phenomena, in which the χT value of the HT phase is larger than that of the LT phase because the entropically favored HS state is the HT phase. The WFe charge-transfer complex without spin transition therefore exhibits a different type of temperature-dependent magnetic behaviour. Magnetization switching through photoinduced charge transfer has also been reported in many cyanide-bridged MoCu systems, which convert from Mo^{IV}–CN–Cu^{II} to Mo^{V}–CN–Cu^{I} (refs 60–62), although the mechanism in MoCu systems is still controversial.

Another type of charge transfer, that between a metal centre and a redox-active ligand within a metal complex, has also been observed — and is usually referred to as valence tautomerism (or redox isomerism)[3,63]. Although most valence tautomeric complexes are comprised of 3*d* transition metals, this behaviour has also been observed in the rare-earth metal complex [{(dpp-bian)Yb(μ-Cl)(1,2-dimethoxyethane)}$_2$] (dpp-bian = 1,2-bis[(2,6-diisopropylphenyl)imino]acenaphthene) (Fig. 2b)[64]. Because of the metal-to-ligand charge transfer, the redox state of the metal centres in the dinuclear Yb_2 complex changes from $Yb^{III}Yb^{III}$ at LT to $Yb^{III}Yb^{II}$ at HT. This Yb complex also displays a reverse thermal hysteresis (ΔT = 7 K) as the magnetic moment decreases from 6.6 to 5.2 μ_B upon heating (transition temperature ≈ 150 K) and returns back to 6.6 μ_B after cooling (Fig. 4b).

Because a diverse range of metals, including lanthanides, and of organic molecules can also be used in charge-transfer systems, a great variety of dynamic crystals based on this phenomenon is expected to be developed, by choosing donors and acceptors with appropriate redox potentials.

Coupled charge transfer and spin transition

Charge transfer can also be coupled with spin transition, and used to induce dynamic change in molecular compounds. In this process — referred to as charge- (or electron-) transfer-coupled spin transition (CTCST or ETCST) or charge-transfer-induced spin transition (CTIST) — the configuration of a metal centre changes from high to low spin, or vice versa, with the charge transfer[4].

The ligand field splitting tends to increase with increasing oxidation number of central metal ions. Therefore, when the ligand field in a charge-transfer system is just within the conditions of a

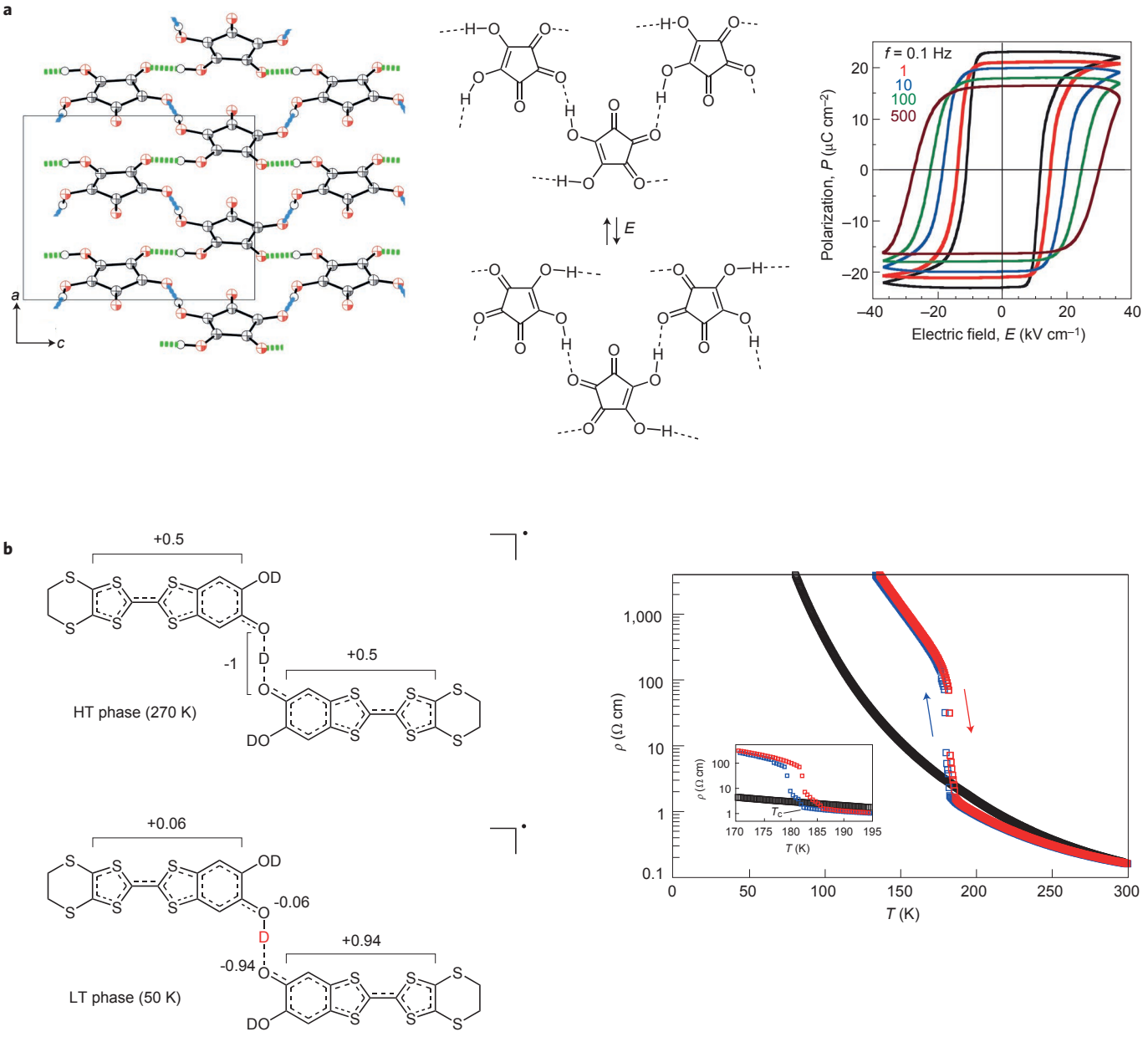

Figure 6 | Control of physical properties through the induction of proton transfer. a, Left, crystal structure of croconic acid. Middle, schematic of the polarization reversal mechanism. Right, polarization versus electric field plots measured with an alternating current electric field at frequency f ranging from 0.1 to 500 Hz (ref. 93). **b**, Left, chemical structures of the hydrogen-bonded molecular unit in κ-D_3(Cat-EDT-TTF)$_2$ at 270 K and 50 K (ref. 100). Two crystallographically equivalent Cat-EDT-TTF$^{+0.5}$ skeletons are linked by a symmetric [O···D···O]$^{-1}$ hydrogen bond at 270 K, whereas charge-poor Cat-EDT-TTF$^{+0.06}$ and charge rich Cat-EDT-TTF$^{+0.94}$ are linked by an asymmetric O$^{-0.06}$–D···O$^{-0.94}$ hydrogen bond at 50 K. Right, temperature dependence of electrical resistivity of κ-D_3(Cat-EDT-TTF)$_2$ (blue = cooling process, red = heating process) and κ-H_3(Cat-EDT-TTF)$_2$ (black = cooling process)[100]. Figure reproduced from 93, NPG (**a**, left and right); and ref. 100, American Chemical Society (**b**).

HS state for a low oxidation state (for example, +2) and LS state for a high oxidation state (for example, +3), coupled charge transfer and spin transition can be observed. Note that ETCST is also a type of valence tautomerism (redox isomerism). The metal-to-metal charge transfer, which is coupled to spin transition, in coordination compounds was extensively investigated for cyanide-bridged coordination polymers such as FeCo, WCo, and OsCo systems[5,62,65,66]. The FeCo Prussian blue analogue with a three-dimensional Fe–CN–Co structure was the first example of a molecular photomagnet[4,67–69], and phototunable FeCo single-chain magnets with a one-dimensional Fe–CN–Co structure have also been reported[70–72].

Recently various multinuclear cyanide-bridged FeCo clusters exhibiting thermal and photoinduced charge transfers have also been synthesized[73–78]. The charge transfer process of FeCo compounds is expressed through a reversible phase transition between low-temperature phase with $Fe^{II}_{LS(S=0)}$–CN–$Co^{III}_{LS(S=0)}$ and a high-temperature phase with $Fe^{III}_{LS(S=1/2)}$–CN–$Co^{II}_{HS(S=3/2)}$ (Fig. 2c). This phase transition is driven by entropy originating from both ΔS^{etp}_{el} and ΔS^{etp}_{vib}, and the temperature at which it occurs can be tuned by controlling the redox potential of either the Co or the Fe ion, through modifications of their coordination ligands[75]. The Co^{II}_{HS} complex has a larger molecular volume than its Co^{III}_{LS} counterpart because it comprises two electrons occupying the e_g orbital with anti-bonding character. These structural changes at the molecular level induce crystal deformation during the phase transition[33].

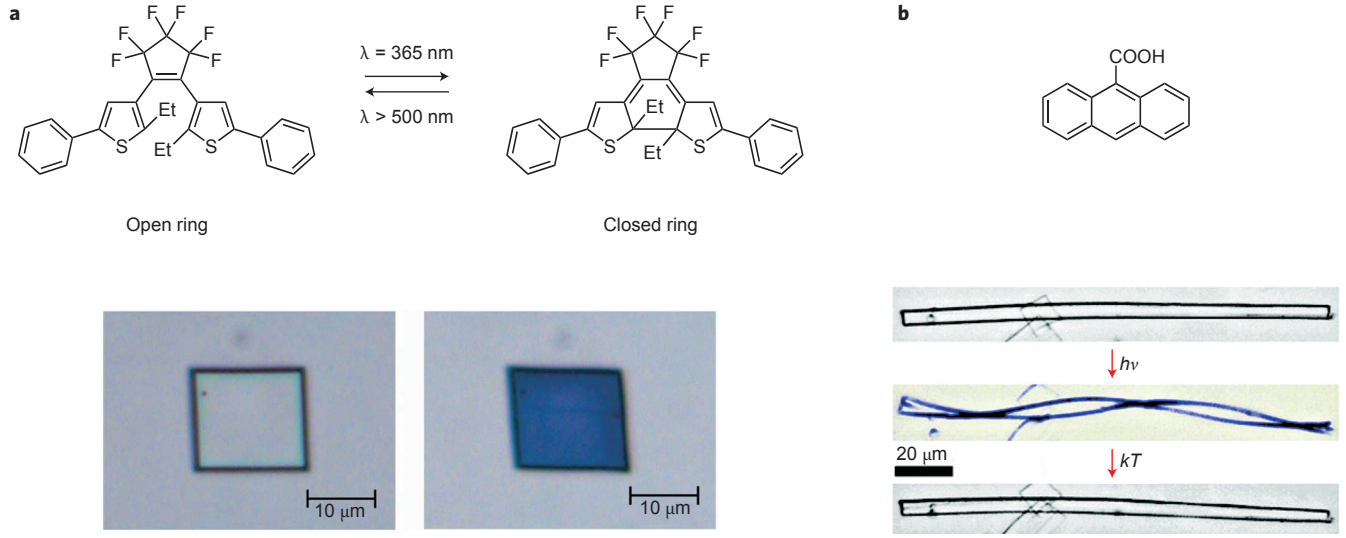

Figure 7 | Control of physical properties through the induction of molecular structural change. a, Molecular structures of the open- and closed-ring isomers of a diarylethene compound, 1,2-bis(2-ethyl-5-phenyl-3-thienyl)perfluorocyclopentene, and single crystal deformation upon irradiation with ultraviolet and visible light; a square single crystal with corner angles of 88° and 92° reversibly changed to a lozenge shape with corner angles of 82° and 98° (ref. 105). **b**, Molecular structure of 9-anthracenecarboxylic acid and reversible photoinduced twisting of its crystal[108]. Figure reproduced from ref. 105, NPG (**a**); and ref. 108, American Chemical Society (**b**).

A recent noteworthy achievement is the preparation of phototunable SMM, $[Co_2Fe_4(bimpy)_2(CN)_6(\mu\text{-}CN)_6(pztp)_4]\cdot 2(1\text{-}PrOH)\cdot 4H_2O$ (bimpy = 2,6-bis(benzimidazol-2-yl)pyridine, pztp = tetrakis(1-pyrazolyl)borate) (Fig. 5a)[29]. The Fe_4Co_2 hexanuclear compound exhibits thermal charge transfer. The redox state of the metal centres changes from $[Fe^{III}_{LS}\{(Co^{II}_{HS})_2(Fe^{III}_{LS})_2\}Fe^{III}_{LS}]$ (HT phase) to $[Fe^{III}_{LS}\{(Co^{III}_{LS})_2(Fe^{II}_{LS})_2\}Fe^{III}_{LS}]$ (LT phase). When the LT phase compound is irradiated with 808 nm light to excite the charge transfer band from Fe^{II}_{LS} to Co^{III}_{LS}, a photoinduced metastable state — assigned the same electronic structure as that of the HT phase — exhibits slow relaxation of magnetization, suggesting that it behaves as an SMM (ref. 29).

Charge transfer coupled with spin transition has also been observed in several other cyanide-bridged heterobimetallic complexes[79–80]. In particular, unusual charge transfer was observed in a trimetallic cyanide-bridged cluster, $\{Co^{II}_3Fe^{II}_6[W^{V}(CN)_8]_6(MeOH)_{24}\}\cdot x$MeOH (Fig. 5b)[80], which has two active electron-transfer channels. One is the transition $W^{IV}_{(S=0)}$–CN–$Co^{III}_{LS(S=0)}$ (LT phase) ⇆ $W^{V}_{(S=1/2)}$–CN–$Co^{II}_{HS(S=3/2)}$ (HT phase). Additionally, a charge transfer can also occur without spin transition between W and Fe ions, which is expressed by $W^{IV}_{(S=0)}$–CN–$Fe^{III}_{HS(S=5/2)}$ (LT phase) ⇆ $W^{V}_{(S=1/2)}$–CN–$Fe^{II}_{HS(S=2)}$ (HT phase). The overall change in the redox state is shown in Fig. 5b. These concomitant charge-transfer processes endow the cluster with thermal bistability.

Numerous metal complexes with redox-active ligands such as catechol and semiquinone ligands also exhibit charge transfer between a metal centre and a ligand that involves a spin transition in the metal[3,63]. As described above, the charge transfer between a metal and a ligand, regardless of whether it involves a spin transition, is typically called valence tautomerism. It can be induced by changes in temperature or pressure, and is accompanied by changes in the magnetic and optical properties of the complex[3,25,63,81,82]. In the presence of strong intermolecular interactions, the temperature-dependent magnetic behaviour shows an abrupt change with hysteresis[83].

Valence tautomerism in cobalt complexes can also be induced by exposure to visible light or soft X-ray[81,82,84]. Photoinduced valence tautomerism has been observed within crystals as well as diluted in a rigid-glass matrix[82]. This means that cobalt valence tautomeric complexes can potentially be combined with other functional molecules, as in spin-crossover complexes, and serve as thermal- and photo-tunable molecular units within crystalline compounds to modulate various physical properties, such as conductivity. Notably, an interesting phenomenon reported in a cobalt compound is that of a photoinduced crystal bending[85]; an even larger photomechanical effect reported has also been observed in a rhodium compound[86].

Proton transfer

Proton transfer events play an important role in biological systems, and also drive interesting reversible behaviours in molecular materials[6,7]. For example, the 4,4′-bipyridinium salt of squaric acid exhibits a colour change that arises from temperature-induced proton transfer[87,88]. Similarly, proton transfer processes have also been involved in pressure-induced colour changes[87,88] and mechanochromism (a change of colour under mechanical stress)[89].

Furthermore, proton transfer is a key mechanism in some molecular ferroelectric compounds — which exhibit a spontaneous and electrically reversible polarization[90–95]. This phenomenon in a two-component system typically involves an acid and a base, and a proton shuttling between them[91]. In an electric field, the migration of a proton between the two components changes their polarization, thus inducing a switch in the electric polarity of the material and giving rise to ferroelectricity. Recently a ferroelectric behaviour arising from an intermolecular proton transfer has been identified in a single-component system, crystalline croconic acid, owing to a keto–enol tautomerization. Croconic acid crystals showed ferroelectric behaviour at high temperatures (400 K; ref. 93), and also showed the highest spontaneous polarization reported so far (about 20 μC cm^{-2}) in organic ferroelectrics (Fig. 6a). Following this study, various other ferroelectric organic components have been identified, such as 2-methylbenzimidazole whose ferroelectricity arises from the imidazole motif, wherein the polarity inversion is induced by proton tautomerism involving proton transfer and concomitant π-bond switching (Fig. 2d)[94].

Proton transfer coupled with electron transfer is also observed in biological systems[96] — photosynthesis for example involves the transfer of no less than 24 electrons and 24 protons. Many attempts have been made to couple these two events in solid-state compounds. Cooperative proton–electron transfer has been reported for several

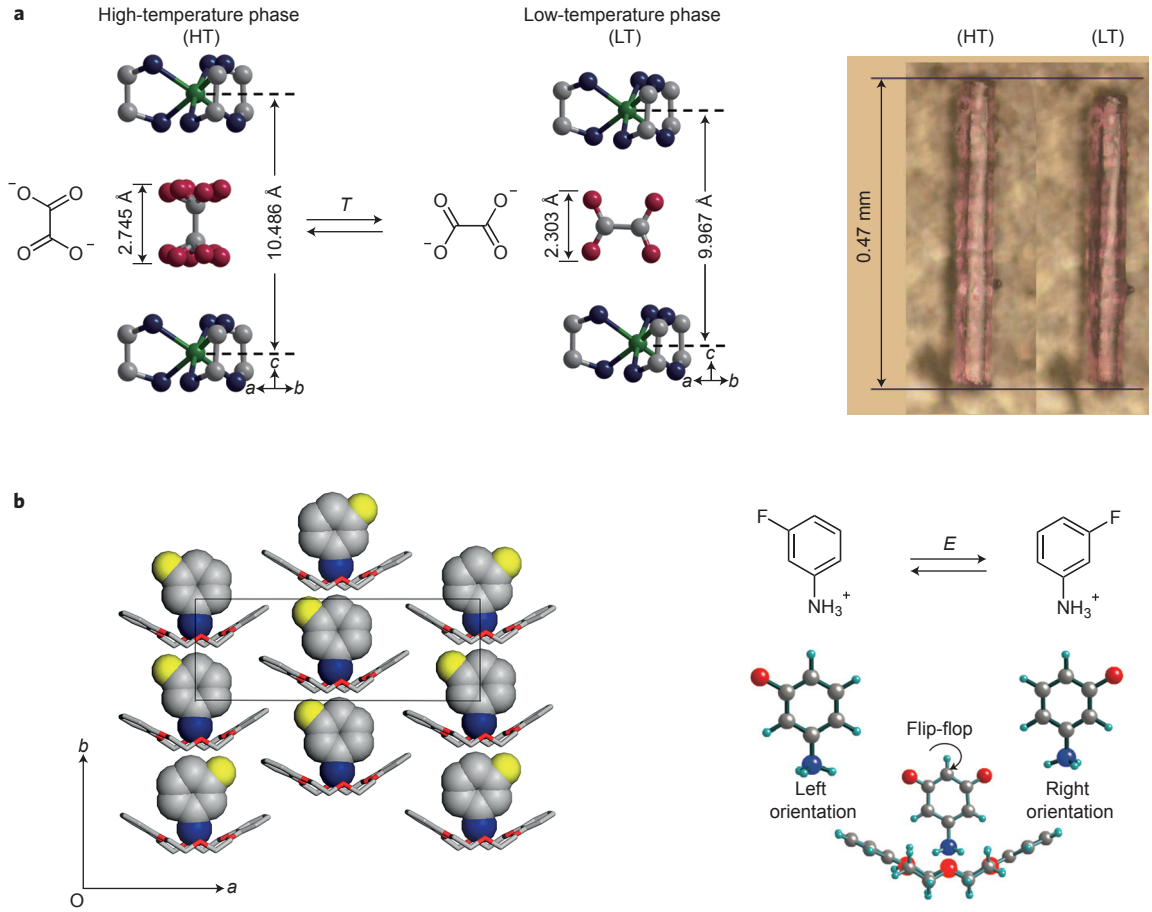

Figure 8 | Control of physical properties through the induction of molecular orientation change. a, Crystal deformation of $[Ni^{II}(en)_3](ox)$ induced by oxalate reorientation. Left, distance between Ni ions and the oxalate dianion height measured at HT are 10.486 Å and 2.745 Å, respectively (263 K on cooling), and the distance between Ni ions and the oxalate dianion height measured at LT are 9.967 Å and 2.303 Å, respectively (243 K on cooling). Upon cooling, the distance between Ni ions decreases by 4.9% along the crystallographic *c* axis with a 90° rotation of oxalate molecules. Green (Ni), blue (N), red (O) and grey (C). Right, photographs of crystal deformation recorded at 254 K (HT) and 253 K (LT) on cooling. The sample contracted along the long axis of the order of 5% during cooling, which mainly reflects the change in the distance between Ni ions along the crystallographic *c* axis, because the long axis of the crystal is parallel to the crystallographic *c* axis[126]. **b**, Supramolecular rotator layer (left) and average structure (right) of (*m*-$FANi^+$)(DB[18]crown-6) (ref. 129). An external electric field reverses the direction of the dipole moment. Figure reproduced from ref. 126, NPG (**a**); and ref. 129, NPG (**b**).

organic co-crystals[97,98], for example between a *p*-benzoquinone and its corresponding hydroquinone. More recently, synergy between proton dynamics and conductivity, and between proton dynamics and magnetization, have been observed in a hydrogen-bonded molecular crystal (Fig. 6b)[99,100]. The conducting organic crystal κ-D_3(Cat–EDT–TTF)$_2$ (Cat–EDT–TTF = catechol-fused ethylenedithiotetrathiafulvalene, D = deuterium) undergoes a phase transition at 185 K, where deuterium transfer occurs along the hydrogen bond pathway and is accompanied by electron transfer between the Cat–EDT–TTF molecules (Fig. 6b). When cooled below room temperature, the paramagnetic semiconductor with a dimer-Mott-type electronic structure converts into a nonmagnetic insulator with a charge-ordered electronic structure. Figure 6b shows that, upon cooling, the resistivity abruptly increases at the phase transition temperature. It should be noted that the non-deuterated parent compound, κ-H_3(Cat–EDT–TTF)$_2$, does not show this semiconductor–insulator-like phase transition, but exhibits continuous monotonic semiconducting behaviour. This is attributed to the isotope effect on the geometry and potential energy curve of the hydrogen bond.

Proton-transfer processes are very versatile because suitable sites can be introduced into numerous organic molecules and coordination compounds (in ligands), this makes them promising for the rational preparation of functional materials.

Change in molecular structure

Many molecules are known to undergo structural changes triggered thermally or by light irradiation[8–11], or through the application of pressure[101,102]. Changes in a molecular structure are in turn accompanied by a modification of its electronic structure, through a change in the electron distribution in the molecule. Thus, molecular-level structural changes in crystalline compounds inevitably cause dynamic changes in their properties.

The most extensively studied molecular systems that undergo external stimuli-induced structural changes are photochromic molecules, which exhibit reversible conversion between two isomers under light irradiation. The two isomers exhibit different absorption spectra, and hence different optical properties. Such photochromic molecules have been widely used to switch various properties of molecular crystals[8,103].

Typical examples of photochromic molecules include diarylethene and its derivative compounds, which adopt a closed or an open form (Fig. 7a, top)[8]. Photoisomerization of many diarylethene derivatives can be induced in the crystalline state, depending on the conformation of the molecule within the crystal[104]. Recently, rapid and reversible shape changes in diarylethene crystals have been observed[105]. The change between the open and closed forms of the diarylethene unit affects the shapes or sizes of their single

crystals substantially enough to be observed at the macroscopic scale (Fig. 7a, bottom). This change of shape can be triggered on one side of the crystal only, leading to photoinduced crystal bending. A similar crystal bending behaviour was observed for 9-anthracenecarboxylic acid (Fig. 2e), which exhibits photoinduced cycling, and azobenzene molecules, which undergo *cis–trans* photoisomerization[106,107]. Recently, reversible photoinduced twisting of molecular crystals has also been observed, in both 9-anthracenecarboxylic acid (Fig. 7b) and diarylethene[108,109].

Photoinduced molecular structure changes have also been observed in several coordination compounds, through linkage isomerization, and ligand isomerization mechanisms[9,28,110]. In linkage isomers, the same ligand can (and does) coordinate the central metal through different atoms[9,110]. A typical example is sodium nitroprusside $Na_2[Fe(CN)_5NO]\cdot 2H_2O$ (ref. 9). When the complex is irradiated at low temperature, the Fe–NO structure changes to the Fe–ON configuration or the side-on bonded type structure (corresponding to a 180° or 90° rotation of the NO moiety, respectively)[111]. The resulting photoinduced metastable state can only be trapped below room temperature. In contrast, in ligand isomerization the ligand itself undergoes isomerization, with no changes to the atom coordinating to the metal centre. Such a photochromic behaviour has been observed for example in a crystalline organorhodium dithionite complex with photoresponsive dithionite group (μ-O_2SSO_2), $[(RhCp^\star)_2(\mu\text{-}CH_2)_2(\mu\text{-}O_2SSO_2)]$ ($Cp^\star$ = η^5-C_5Me_5) (refs 112,113). When the Rh complex is irradiated with 385–740 nm light, the (μ-O_2SSO_2) ligand is converted to a (μ-O_2SOSO) one. A colour change from red-orange to yellow-orange is observed along with a slight expansion (about 1%) in the volume of the unit cell.

Coordination complexes with photo-switchable properties can thus be engineered through ligand isomerization, by using photoresponsive molecules exhibiting a structural change as ligands. For example, using diarylethene as a ligand in a SMM complex resulted in a SMM whose magnetic behaviour was reversibly controlled by photoisomerization[28]. The realization of photoinduced SMM behaviour in a crystal — where molecules are closely packed — is essential for the application of SMM to high-density photomagnetic recording media. The nitroprusside compound mentioned above also introduced into a cyanide-bridged network structure, in which it served to optically modulate magnetic interaction[114].

Thermally induced structural changes have also been observed in numerous molecular compounds, often involving significant change in physical properties such as optical, or mechanical. In the pseudorotaxane [(*N*-(xylylammonium)-methylferrocene)(DB24C8)](PF_6) (DB24C8 = dibenzo[24]crown-8), a conformational change was observed at the phase-transition temperature[115]. This molecular crystal exhibits significant thermochromic behaviour, where the colour changes from green (LT phase) to orange (HT phase), and is accompanied by an anisotropic change in the crystal's optical properties. Characterization of the compounds by single crystal X-ray diffraction showed that the colour change is accompanied by a thermally induced crystal deformation: at the phase-transition temperature, upon heating the *b* axis expands by 7.3% and the *c* axis contracts by 4%.

In coordination compounds, thermally induced distortion of the coordination environment around a metal centre can also induce the modification of the compound's polarization and magnetic properties. Recently, a ferroelectric compound, $Ca(NO_3)_2$(15-crown-5), with a transition temperature of 205 K, was developed[116], in which the ferroelectricity mechanism was attributed to the coordination distortion of the central calcium atom. Furthermore, in $[Co(NO_3)_2$(2,6-di(pyrazol-1-yl)pyrazine)], the distortion in coordination environment around the Co^{II} centre was observed to modify the splitting of the *d*-orbital, in turn inducing a change in the orbital contribution to the magnetization[117] and resulting in an abrupt switching of the magnetization with hysteresis. In a Cu^{II}-nitroxide cluster, $[Cu(hfac)_2]_4L_2$, (hfac = hexafluoroacetylacetonato, L = 2-(3-pyridyl)-4,4,5,5-tetramethyl-4,5-dihydrlo-1*H*-imidazolyl-1-oxy-3-oxide), a thermally induced switch between HS (six $S = 1/2$ spins) and LS (two $S = 1/2$ spins) was observed[118]. The spin-transition-like behaviour arises from the change in the magnetic interaction between Cu^{II} and the nitroxide radical, which is derived from an equatorial–axial conversion of coordination of an oxyl oxygen in the Cu^{II}–nitroxide cluster[119]. Recently, 1D Cu^{II}–nitroxide compounds have also been found to exhibit a LIESST-like effect[120,121]. Devising a different type of photomagnetic complex would be important for the exploration of new materials applicable to future photomemory devices.

Change in molecular orientation

A change in the molecular orientation of crystals that occurs without significant change in the molecular structure itself can also alter the physical properties of crystalline materials[11,12,122]. Although molecular movement is restricted in the solid state, molecules in crystals can still undergo displacement and rotational motion[123,124]. Furthermore, their orientation exhibits transition between the frozen state and dynamically disordered state, which can lead to changes in the properties of crystals — for example mechanical and ferroelectric ones.

The typical mechanical response of materials under temperature changes is thermal expansion, but unusual thermomechanical properties may be observed through changes in molecular orientation within crystals. Dumbbell-shaped molecules (*S*,*S*)-octa-3,5-diyn-2,7-diol, for example, stack along the crystallographic *a* axis, where the angle of the diyne spines relative to the stacking direction is 54.2° at 225 K (ref. 125). Upon heating, the stacking angle changes to 51.0° at 330 K. This change in molecular orientation results in an anisotropic and gradual crystal deformation with temperature; exceptionally large uniaxial (*a* axis) positive thermal expansion and biaxial (*b* and *c* axes) negative thermal expansion of the crystal. In contrast to this gradual change, abrupt and anisotropic crystal deformation was observed in a crystalline Ni complex, $[Ni^{II}(en)_3](ox)$ (en = ethylenediamine and ox = oxalate anion), where cooperativity was derived from intermolecular hydrogen bonding (Fig. 8a)[126]. Single-crystal X-ray diffraction analysis showed that 90° molecular rotation of the oxalate molecules (Fig. 2f) in the crystal induced a size change on the order of 0.4 Å per molecule in the *c* axis direction. The change in subnanometre size induced by a molecular scale rotor is amplified to contraction/expansion at a micrometre scale along the long axis of the crystal due to the collective motion of molecules in the whole crystal through cooperative interactions. The size change of the crystal can be clearly observed under an optical microscope (Fig. 8a, right). Such amplification from the nanometre to micrometre scale via a concerted process is reminiscent of muscles in biological systems.

As mentioned above when describing the unusual example of the TTF–CA charge-transfer compound, polarization can be induced in crystals through the displacement of cationic and anionic component from their symmetric positions, resulting in ferroelectric properties. An example of such displacive-type ferroelectrics is 4-(cyanomethyl)anilinium perchlorate[127]. This compound exhibits second-order phase transition from a paraelectric phase to a ferroelectric phase at 184 K, where the displacement of 4-(cyanomethyl)anilinium cations and perchlorate anions occur in the crystal. A characteristic of this compound is the observation of a ferroelectric hysteresis loop even at a high frequency of 10 kHz.

Another important mechanism behind ferroelectric phase transitions involves order–disorder transitions. Numerous order–disorder-type ferroelectric compounds have recently been reported[12,128]. In an (*m*-FAni)(dibenzo[18]crown-6)[Ni(dmit)$_2$] crystal, *m*-$FAni^+$ (*m*-$FAni^+$ = *m*-fluoroanilinium) molecules undergo dynamic rotational motion (Fig. 8b)[129]. The molecular motion of *m*-$FAni^+$ is frozen at low temperature, whereas a 180° flip-flop motion of the supramolecular rotator, *m*-$FAni^+$, takes place at high temperature,

where thermal energy overcomes the potential energy barrier of the two structures. When an electric field is applied to a single crystal, the dipole rotation is induced through the 180° rotation of *m*-FAni$^+$ (Fig. 2f). A polarization–electric field dependence at 298 K measured below its ferroelectric phase transition temperature (346 K) shows hysteresis behaviour. The chemically designed dipole unit is used to realize ferroelectricity. Note that the piezoelectric effect (where application of mechanical force induces electric polarity) and the inverse piezoelectric effect (where application of electric field induces mechanical strain) are observed in ferroelectric compounds[130].

Although only mechanical and ferroelectric properties were introduced in the present section, a change in molecular orientation within a crystal can also be used to control many other functions[131,132]. The challenge is the elucidation of a strategy to purposely induce such orientational changes within crystals.

Summary and outlook

Numerous molecular compounds have recently been developed whose magnetic, conductive, ferroelectric, optical, and mechanical properties can be rationally controlled. The precise control of electron-, proton- (atom), and molecular-transfer from one site to another in molecular crystals under external stimuli is essential in switching the crystals' physical properties. Furthermore, changes in crystals' properties can be achieved by introducing tunable molecules that undergo structural change, such as diarylethene as discussed above.

The design of a system that will undergo reversible conversion between two isomers requires that the isomers have nearly equivalent energies. Several parameters, such as ligand field, redox potential, and acidity constant, are useful in controlling the energy level of the isomers. In the case of thermal switching, the entropy term also needs to be carefully considered, as an entropically favourable state is realized at high temperature as a result of the thermodynamics ($G = H - TS^{etp}$, where G is the Gibbs free energy and H the enthalpy). For example, thermally induced spin crossover only occurs when the enthalpy of the entropically favourable high-spin state is slightly higher than that of the low-spin state. The design of compounds displaying dynamic changes in molecular orientation through which the physical properties are greatly modified is a challenging crystal engineering undertaking. Consulting the literature for information on phase transitions in terms of thermodynamics is useful for the design of dynamic crystalline materials[133]. Furthermore, in the case of crystalline materials, molecular interactions play an essential role in the dynamic process. Intermolecular interactions can be strengthened by introducing hydrogen bonds, π-π interaction, and coordinate bonds between molecules.

Many more interesting properties are expected to be accessed in molecular compounds in the near future. The control of physical properties through external stimuli shown in this Review can be applied to the development of various dynamic materials. Photoinduced charge transfer within the crystal, and photoinduced molecular structural changes, can be used to control various functions such as superconducting and ferroelectric properties. Reversible photoinduced charge transfer can also serve to control the polarization in a polar compound; the switching speed achieved using charge transfer is faster than that arising from ion displacements.

The combination of two or more approaches may give access to other, or improved, functional materials. The electrical control of proton transfer and molecular displacement is a common phenomenon in ferroelectric compounds. Exerting a similar control through the application of an external electric field to control the magnetic and optical properties of materials is also attractive. For example, if both intermolecular proton transfer in ligands and proton-dependent ligand fields were simultaneously engineered in the design of dynamic coordination crystals, proton transfer coupled spin transition may be achieved in crystalline state.

Additionally, it is important to investigate the minimum size of crystals that can exhibit bistability through intermolecular interactions in each molecular system[134]. Synthesizing uniform dynamic crystals with the optimum size for bistability is a challenge. The preparation of nanosized crystal via top-down approaches always leads to the generation of size distributions, and methods to synthesize nanosized functional crystals via bottom-up approaches have not been fully explored yet.

Notably, biological systems often contain molecular assemblies exhibiting dynamic properties[135], and their dynamic properties have typically remained much more complex than those so far achieved in synthetic systems. These can help guide chemists on the way to the successful preparation of dynamic molecular crystals with switchable functions that will find applications in molecular devices[136].

Received 9 April 2015; accepted 9 May 2016;
published online 21 June 2016

References

1. Halcrow, M. A. (ed.) *Spin-Crossover Materials: Properties and Applications* (Wiley, 2013).
2. Bousseksou, A., Molnár, G., Salmon, L. & Nicolazzi, W. Molecular spin crossover phenomenon: recent achievements and prospects. *Chem. Soc. Rev.* **40,** 3313–3335 (2011).
3. Tezgerevska, T., Alley, K. G. & Boskovic, C. Valence tautomerism in metal complexes: Stimulated and reversible intramolecular electron transfer between metal centers and organic ligands. *Coord. Chem. Rev.* **268,** 23–40 (2014).
4. Dunbar, K. R., Achim, C. & Shatruk, M. in *Spin-Crossover Materials: Properties and Applications* (ed. Halcrow, M. A.) 171–202 (Wiley, 2013).
5. Sato, O., Tao, J. & Zhang, Y. Z. Control of magnetic properties through external stimuli. *Angew. Chem. Int. Ed.* **46,** 2152–2187 (2007).
6. Morita, Y., Murata, T. & Nakasuji, K. Cooperation of hydrogen-bond and charge-transfer interactions in molecular complexes in the solid state. *Bull. Chem. Soc. Jap.* **86,** 183–197 (2013).
7. Saito, G. & Yoshida, Y. Development of conductive organic molecular assemblies: organic metals, superconductors, and exotic functional materials. *Bull. Chem. Soc. Jap.* **80,** 1–137 (2007).
8. Irie, M., Fukaminato, T., Matsuda, K. & Kobatake, S. Photochromism of diarylethene molecules and crystals: memories, switches, and actuators. *Chem. Rev.* **114,** 12174–12277 (2014).
9. Coppens, P., Novozhilova, I. & Kovalevsky, A. Photoinduced linkage isomers of transition-metal nitrosyl compounds and related complexes. *Chem. Rev.* **102,** 861–883 (2002).
10. Vogelsberg, C. S. & Garcia-Garibay, M. A. Crystalline molecular machines: function, phase order, dimensionality, and composition. *Chem. Soc. Rev.* **41,** 1892–1910 (2012).
11. Nath, N. K., Panda, M. K., Sahoo, S. C. & Naumov, P. Thermally induced and photoinduced mechanical effects in molecular single crystals—a revival. *CrystEngComm* **16,** 1850–1858 (2014).
12. Zhang, W. & Xiong, R. G. Ferroelectric metal–organic frameworks. *Chem. Rev.* **112,** 1163–1195 (2012).
13. Moonen, N. N. P., Flood, A. H., Fernández, J. M. & Stoddart, J. F. in *Topics in Current Chemistry* Vol. **262**, 99–132 (Springer, 2005).
14. Kahn, O. *Molecular Magnetism* (VCH, 1993).
15. Ogawa, Y. *et al.* Dynamical aspects of the photoinduced phase transition in spin-crossover complexes. *Phys. Rev. Lett.* **84,** 3181–3184 (2000).
16. Gutlich, P., Hauser, A. & Spiering, H. Thermal and optical switching of iron(II) complexes. *Angew. Chem. Int. Ed. Engl.* **33,** 2024–2054 (1994).
17. Sorai, M. Calorimetric investigations of phase transitions occurring in molecule-based materials in which electrons are directly involved. *Bull. Chem. Soc. Jap.* **74,** 2223–2253 (2001).
18. Kahn, O. & Martinez, C. J. Spin-transition polymers: from molecular materials toward memory devices. *Science* **279,** 44–48 (1998).
19. Wang, C. F. *et al.* Synergetic spin crossover and fluorescence in one-dimensional hybrid complexes. *Angew. Chem. Int. Ed.* **54,** 1574–1577 (2015).
20. Bonhommeau, S. *et al.* Photoswitching of the dielectric constant of the spin-crossover complex $[Fe(L)(CN)_2]\cdot H_2O$. *Angew. Chem. Int. Ed.* **45,** 1625–1629 (2006).
21. Decurtins, S., Gutlich, P., Kohler, C. P., Spiering, H. & Hauser, A. Light-induced excited spin state trapping in a transition-metal complex: the hexa-1-propyltetrazole-iron(II) tetrafluoroborate spin-crossover system. *Chem. Phys. Lett.* **105,** 1–4 (1984).

22. Hayami, S. *et al.* First observation of light-induced excited spin state trapping for an iron(III) complex. *J. Am. Chem. Soc.* **122,** 7126–7127 (2000).
23. Ohkoshi, S. I., Imoto, K., Tsunobuchi, Y., Takano, S. & Tokoro, H. Light-induced spin-crossover magnet. *Nature Chem.* **3,** 564–569 (2011).
24. Linares, J., Codjovi, E. & Garcia, Y. Pressure and temperature spin crossover sensors with optical detection. *Sensors* **12,** 4479–4492 (2012).
25. Gütlich, P., Gaspar, A. B., Garcia, Y. & Ksenofontov, V. Pressure effect studies in molecular magnetism. *Compt. Rend. Chimie* **10,** 21–36 (2007).
26. Gatteschi, D. & Sessoli, R. Quantum tunneling of magnetization and related phenomena in molecular materials. *Angew. Chem. Int. Ed.* **42,** 268–297 (2003).
27. Parois, P. *et al.* Pressure-induced Jahn–Teller switching in a Mn_{12} nanomagnet. *Chem. Commun.* **46,** 1881–1883 (2010).
28. Morimoto, M., Miyasaka, H., Yamashita, M. & Irie, M. Coordination assemblies of $[Mn_4]$ single-molecule magnets linked by photochromic ligands: photochemical control of the magnetic properties. *J. Am. Chem. Soc.* **131,** 9823–9835 (2009).
29. Nihei, M. *et al.* A light-induced phase exhibiting slow magnetic relaxation in a cyanide-bridged Fe_4Co_2 complex. *Angew. Chem. Int. Ed.* **51,** 6361–6364 (2012).
30. Feng, X. *et al.* Tristability in a light-actuated single-molecule magnet. *J. Am. Chem. Soc.* **135,** 15880–15884 (2013).
31. Mathonière, C., Lin, H. J., Siretanu, D., Clérac, R. & Smith, J. M. Photoinduced single-molecule magnet properties in a four-coordinate iron(II) spin crossover complex. *J. Am. Chem. Soc.* **135,** 19083–19086 (2013).
32. Liu, T. *et al.* A light-induced spin crossover actuated single-chain magnet. *Nature Commun.* **4,** 2826 (2013).
33. Shepherd, H. J. Molecular actuators driven by cooperative spin-state switching. *Nature Commun.* **4,** 3607 (2013).
34. Dorbes, S., Valade, L., Real, J. A. & Faulmann, C. $[Fe(sal_2\text{-trien})][Ni(dmit)_2]$: towards switchable spin crossover molecular conductors. *Chem. Commun.* 69–70 (2005).
35. Takahashi, K. *et al.* Evidence of the chemical uniaxial strain effect on electrical conductivity in the spin-crossover conducting molecular system: $[Fe^{III}(qnal)_2][Pd(dmit)_2]_5$·acetone. *J. Am. Chem. Soc.* **130,** 6688–6689 (2008).
36. Phan, H., Benjamin, S. M., Steven, E., Brooks, J. S. & Shatruk, M. Photomagnetic response in highly conductive iron(II) spin-crossover complexes with TCNQ radicals. *Angew. Chem. Int. Ed.* **54,** 823–827 (2015).
37. Hicks, R. G. A new spin on bistability. *Nature Chem.* **3,** 189–191 (2011).
38. Ratera, I. & Veciana, J. Playing with organic radicals as building blocks for functional molecular materials. *Chem. Soc. Rev.* **41,** 303–349 (2012).
39. Fujita, W. & Awaga, K. Room-temperature magnetic bistability in organic radical crystals. *Science* **286,** 261–262 (1999).
40. Vela, S. *et al.* The key role of vibrational entropy in the phase transitions of dithiazolyl-based bistable magnetic materials. *Nature Commun.* **5,** 4411 (2014).
41. Pal, S. K. *et al.* Hysteretic spin and charge delocalization in a phenalenyl-based molecular conductor. *J. Am. Chem. Soc.* **132,** 17258–17264 (2010).
42. Lekin, K. *et al.* Hysteretic spin crossover between a bisdithiazolyl radical and its hypervalent σ-dimer. *J. Am. Chem. Soc.* **132,** 16212–16224 (2010).
43. Phan, H., Lekin, K., Winter, S. M., Oakley, R. T. & Shatruk, M. Photoinduced solid state conversion of a radical σ-dimer to a π-radical pair. *J. Am. Chem. Soc.* **135,** 15674–15677 (2013).
44. Lekin, K. *et al.* Heat, pressure and light-induced interconversion of bisdithiazolyl radicals and dimers. *J. Am. Chem. Soc.* **136,** 8050–8062 (2014).
45. Matsumoto, S., Higashiyama, T., Akutsu, H. & Nakatsuji, S. A functional nitroxide radical displaying unique thermochromism and magnetic phase transition. *Angew. Chem. Int. Ed.* **50,** 10879–10883 (2011).
46. Nishimaki, H. & Ishida, T. Organic two-step spin-transition-like behavior in a linear $S = 1$ array: 3′-methylbiphenyl-3,5-diyl bis(*tert*-butylnitroxide) and related compounds. *J. Am. Chem. Soc.* **132,** 9598–9599 (2010).
47. Torrance, J. B., Vazquez, J. E., Mayerle, J. J. & Lee, V. Y. Discovery of a neutral-to-ionic phase transition in organic materials. *Phys. Rev. Lett.* **46,** 253–257 (1981).
48. Horiuchi, S., Kumai, R., Okimoto, Y. & Tokura, Y. Chemical approach to neutral–ionic valence instability, quantum phase transition, and relaxor ferroelectricity in organic charge-transfer complexes. *Chem. Phys.* **325,** 78–91 (2006).
49. Lemée-Cailleau, M. H. *et al.* Thermodynamics of the neutral-to-ionic transition as condensation and crystallization of charge-transfer excitations. *Phys. Rev. Lett.* **79,** 1690–1693 (1997).
50. Torrance, J. B. *et al.* Anomalous nature of neutral-to-ionic phase transition in tetrathiafulvalene-chloranil. *Phys. Rev. Lett.* **47,** 1747–1750 (1981).
51. Kobayashi, K. *et al.* Electronic ferroelectricity in a molecular crystal with large polarization directing antiparallel to ionic displacement. *Phys. Rev. Lett.* **108,** 237601 (2012).
52. Horiuchi, S., Kobayashi, K., Kumai, R. & Ishibashi, S. Ionic versus electronic ferroelectricity in donor-acceptor molecular sequences. *Chem. Lett.* **43,** 26–35 (2014).
53. Miyamoto, T., Yada, H., Yamakawa, H. & Okamoto, H. Ultrafast modulation of polarization amplitude by terahertz fields in electronic-type organic ferroelectrics. *Nature Commun.* **4,** 2586 (2013).
54. Ishihara, S. Electronic ferroelectricity in molecular organic crystals. *J. Phys. Cond. Matter* **26,** 493201 (2014).
55. Monceau, P., Nad, F. Y. & Brazovskii, S. Ferroelectric Mott-Hubbard phase of organic $(TMTTF)_2X$ conductors. *Phys. Rev. Lett.* **86,** 4080–4083 (2001).
56. Yamamoto, K. *et al.* Strong optical nonlinearity and its ultrafast response associated with electron ferroelectricity in an organic conductor. *J. Phys. Soc. Jap.* **77,** 074709 (2008).
57. Chorazy, S. *et al.* Charge transfer phase transition with reversed thermal hysteresis loop in the mixed-valence $Fe_9[W(CN)_8]_6$·*x*MeOH cluster. *Chem. Commun.* **50,** 3484–3487 (2014).
58. Itoi, M. *et al.* Charge-transfer phase transition and ferromagnetism of iron mixed-valence complexes $(n\text{-}C_nH_{2n+1})_4N[Fe^{II}Fe^{III}(dto)_3]$ ($n = 3$–6; dto = $C_2O_2S_2$). *Eur. J. Inorg. Chem.* 1198–1207 (2006).
59. Kojima, N., Itoi, M., Ono, Y., Okubo, M. & Enomoto, M. Spin-entropy driven charge-transfer phase transition in iron mixed-valence system. *Mater. Sci. Poland* **21,** 181–189 (2003).
60. Herrera, J. M. *et al.* Reversible photoinduced magnetic properties in the heptanuclear complex $[Mo^{IV}(CN)_2(CN\text{-}CuL)_6]^{8+}$: a photomagnetic high-spin molecule. *Angew. Chem. Int. Ed.* **43,** 5468–5471 (2004).
61. Bleuzen, A., Marvaud, V., Mathoniere, C., Sieklucka, B. & Verdaguer, M. Photomagnetism in clusters and extended molecule-based magnets. *Inorg. Chem.* **48,** 3453–3466 (2009).
62. Ohkoshi, S. I. & Tokoro, H. Photomagnetism in cyano-bridged bimetal assemblies. *Acc. Chem. Res.* **45,** 1749–1758 (2012).
63. Pierpont, C. G. Studies on charge distribution and valence tautomerism in transition metal complexes of catecholate and semiquinonate ligands. *Coord. Chem. Rev.* **216–217,** 99–125 (2001).
64. Fedushkin, I. L. *et al.* Genuine redox isomerism in a rare-earth-metal complex. *Angew. Chem. Int. Ed.* **51,** 10584–10587 (2012).
65. Sato, O. Optically switchable molecular solids: photoinduced spin-crossover, photochromism, and photoinduced magnetization. *Acc. Chem. Res.* **36,** 692–700 (2003).
66. Avendano, C. *et al.* Temperature and light induced bistability in a $Co_3[Os(CN)_6]_2$ $6H_2O$ prussian blue analog. *J. Am. Chem. Soc.* **132,** 13123–13125 (2010).
67. Sato, O., Iyoda, T., Fujishima, A. & Hashimoto, K. Photoinduced magnetization of a cobalt iron cyanide. *Science* **272,** 704–705 (1996).
68. Verdaguer, M. Molecular electronics emerges from molecular magnetism. *Science* **272,** 698–699 (1996).
69. Bleuzen, A. *et al.* Photoinduced ferrimagnetic systems in Prussian blue analogues $C^I_xCo_4[Fe(CN)_6]_y$ (C^I = alkali cation). 1. Conditions to observe the phenomenon. *J. Am. Chem. Soc.* **122,** 6648–6652 (2000).
70. Liu, T., Zhang, Y. J., Kanegawa, S. & Sato, O. Photoinduced metal-to-metal charge transfer toward single-chain magnet. *J. Am. Chem. Soc.* **132,** 8250–8251 (2010).
71. Dong, D. P. *et al.* Photoswitchable dynamic magnetic relaxation in a well-isolated $\{Fe_2Co\}$ double-zigzag chain. *Angew. Chem. Int. Ed.* **51,** 5119–5123 (2012).
72. Hoshino, N. *et al.* Three-way switching in a cyanide-bridged CoFe chain. *Nature Chem.* **4,** 921–926 (2012).
73. Koumousi, E. S. *et al.* Metal-to-metal electron transfer in Co/Fe Prussian blue molecular analogues: the ultimate miniaturization. *J. Am. Chem. Soc.* **136,** 15461–15464 (2014).
74. Liu, T. *et al.* Reversible electron transfer in a linear $\{Fe_2Co\}$ trinuclear complex induced by thermal treatment and photoirraditaion. *Angew. Chem. Int. Ed.* **51,** 4367–4370 (2012).
75. Nihei, M. *et al.* Controlled intramolecular electron transfers in cyanide-bridged molecular squares by chemical modifications and external stimuli. *J. Am. Chem. Soc.* **133,** 3592–3600 (2011).
76. Zhang, Y. Z. *et al.* Thermochromic and photoresponsive cyanometalate Fe/Co squares: toward control of the electron transfer temperature. *J. Am. Chem. Soc.* **136,** 16854–16864 (2014).
77. Berlinguette, C. P. *et al.* A charge-transfer-induced spin transition in the discrete cyanide-bridged complex $\{[Co(tmphen)_2]_3[Fe(CN)_6]_2\}$. *J. Am. Chem. Soc.* **126,** 6222–6223 (2004).
78. Li, D. F. *et al.* Magnetic and optical bistability driven by thermally and photoinduced intramolecular electron transfer in a molecular cobalt-iron Prussian blue analogue. *J. Am. Chem. Soc.* **130,** 252–258 (2008).
79. Hilfiger, M. G. *et al.* An unprecedented charge transfer induced spin transition in an Fe–Os cluster. *Angew. Chem. Int. Ed.* **49,** 1410–1413 (2010).
80. Podgajny, R. *et al.* Co-NC-W and Fe-NC-W electron-transfer channels for thermal bistability in trimetallic $\{Fe_6Co_3[W(CN)_8]_6\}$ cyanido-bridged cluster. *Angew. Chem. Int. Ed.* **52,** 896–900 (2013).

81. Dei, A., Gatteschi, D., Sangregorio, C. & Sorace, L. Quinonoid metal complexes: toward molecular switches. *Acc. Chem. Res.* **37,** 827–835 (2004).
82. Sato, O., Cui, A. L., Matsuda, R., Tao, J. & Hayami, S. Photo-induced valence tautomerism in Co complexes. *Acc. Chem. Res.* **40,** 361–369 (2007).
83. Tao, J., Maruyama, H. & Sato, O. Valence tautomeric transitions with thermal hysteresis around room temperature and photoinduced effects observed in a cobalt–tetraoxolene complex. *J. Am. Chem. Soc.* **128,** 1790–1791 (2006).
84. Poneti, G. *et al.* Soft-X-ray-induced redox isomerism in a cobalt dioxolene complex. *Angew. Chem. Int. Ed.* **49,** 1954–1957 (2010).
85. Jung, O. S. & Pierpont, C. G. Photomechanical polymers. Synthesis and characterization of a polymeric pyrazine-bridged cobalt semiquinonate–catecholate complex. *J. Am. Chem. Soc.* **116,** 2229–2230 (1994).
86. Abakumov, G. A. & Nevodchikov, V. I. Thermomechanical and photomechanical effects observed on crystals of a free-radical complex. *Doklady Akademii Nauk Sssr* **266,** 1407–1410 (1982).
87. Reetz, M. T., Höger, S. & Harms, K. Proton-transfer-dependent reversible phase changes in the 4,4′-bipyridinium salt of squaric acid. *Angew. Chem. Int. Ed. Engl.* **33,** 181–183 (1994).
88. Martins, D. M. S. *et al.* Temperature- and pressure-induced proton transfer in the 1:1 adduct formed between squaric acid and 4,4-bipyridine. *J. Am. Chem. Soc.* **131,** 3884–3893 (2009).
89. Sheth, A. R., Lubach, J. W., Munson, E. J., Muller, F. X. & Grant, D. J. W. Mechanochromism of piroxicam accompanied by intermolecular proton transfer probed by spectroscopic methods and solid-phase changes. *J. Am. Chem. Soc.* **127,** 6641–6651 (2005).
90. Horiuchi, S. & Tokura, Y. Organic ferroelectrics. *Nature Mater.* **7,** 357–366 (2008).
91. Horiuchi, S., Kumai, R. & Tokura, Y. A supramolecular ferroelectric realized by collective proton transfer. *Angew. Chem. Int. Ed.* **46,** 3497–3501 (2007).
92. Szafrański, M., Katrusiak, A. & McIntyre, G. J. Ferroelectric order of parallel bistable hydrogen bonds. *Phys. Rev. Lett.* **89,** 2155071–2155074 (2002).
93. Horiuchi, S. *et al.* Above-room-temperature ferroelectricity in a single-component molecular crystal. *Nature* **463,** 789–792 (2010).
94. Horiuchi, S. *et al.* Above-room-temperature ferroelectricity and antiferroelectricity in benzimidazoles. *Nature Commun.* **3,** 1308 (2012).
95. Horiuchi, S., Kumai, R., Tokunaga, Y. & Tokura, Y. Proton dynamics and room-temperature ferroelectricity in anilate salts with a proton sponge. *J. Am. Chem. Soc.* **130,** 13382–13391 (2008).
96. Weinberg, D. R. *et al.* Proton-coupled electron transfer. *Chem. Rev.* **112,** 4016–4093 (2012).
97. Nakasuji, K. *et al.* Exploration of new cooperative proton-electron transfer (PET) systems. First example of extended conjugated quinhydrones: 1,5-dihalo-2,6-naphthoquinhydrones. *J. Am. Chem. Soc.* **113,** 1862–1864 (1991).
98. Felderhoff, M., Steller, I., Reyes-Arellano, A., Boese, R. & Sustmann, R. Cooperative proton-electron transfer in a supramolecular structure of *meso*-1,2-bis-(4-dimethylaminophenyl)-1,2-ethanediol and bis(4-cyanobenzylidene) ethylenediamine. *Adv. Mater.* **8,** 402–405 (1996).
99. Isono, T. *et al.* Hydrogen bond-promoted metallic state in a purely organic single-component conductor under pressure. *Nature Commun.* **4,** 1344 (2013).
100. Ueda, A. *et al.* Hydrogen-bond-dynamics-based switching of conductivity and magnetism: A phase transition caused by deuterium and electron transfer in a hydrogen-bonded purely organic conductor crystal. *J. Am. Chem. Soc.* **136,** 12184–12192 (2014).
101. Tomotsune, S. & Sekiya, T. Effect of pressure on photochromic furylfulgide. *Eur. Phys. J. B* **86,** 218 (2013).
102. Iwasa, Y. *et al.* New phases of C_{60} synthesized at high pressure. *Science* **264,** 1570–1572 (1994).
103. Wang, M. S., Xu, G., Zhang, Z. J. & Guo, G. C. Inorganic–organic hybrid photochromic materials. *Chem. Commun.* **46,** 361–376 (2010).
104. Irie, M. Diarylethenes for memories and switches. *Chem. Rev.* **100,** 1685–1716 (2000).
105. Kobatake, S., Takami, S., Muto, H., Ishikawa, T. & Irie, M. Rapid and reversible shape changes of molecular crystals on photoirradiation. *Nature* **446,** 778–781 (2007).
106. Al-Kaysi, R. O. & Bardeen, C. J. Reversible photoinduced shape changes of crystalline organic nanorods. *Adv. Mater.* **19,** 1276–1280 (2007).
107. Koshima, H., Ojima, N. & Uchimoto, H. Mechanical motion of azobenzene crystals upon photoirradiation. *J. Am. Chem. Soc.* **131,** 6890–6891 (2009).
108. Zhu, L., Al-Kaysi, R. O. & Bardeen, C. J. Reversible photoinduced twisting of molecular crystal microribbons. *J. Am. Chem. Soc.* **133,** 12569–12575 (2011).
109. Kitagawa, D., Nishi, H. & Kobatake, S. Photoinduced twisting of a photochromic diarylethene crystal. *Angew. Chem. Int. Ed.* **52,** 9320–9322 (2013).
110. McClure, B. A. & Rack, J. J. Isomerization in photochromic ruthenium sulfoxide complexes. *Eur. J. Inorg. Chem.* 3895–3904 (2010).
111. Schaniel, D. & Woike, T. Necessary conditions for the photogeneration of nitrosyl linkage isomers. *Phys. Chem. Chem. Phys.* **11,** 4391–4395 (2009).
112. Nakai, H. *et al.* Direct observation of photochromic dynamics in the crystalline state of an organorhodium dithionite complex. *Angew. Chem. Int. Ed.* **45,** 6473–6476 (2006).
113. Nakai, H. *et al.* Photochromism of an organorhodium dithionite complex in the crystalline-state: Molecular motion of pentamethylcyclopentadienyl ligands coupled to atom rearrangement in a dithionite ligand. *J. Am. Chem. Soc.* **130,** 17836–17845 (2008).
114. Gu, Z. Z., Sato, O., Iyoda, T., Hashimoto, K. & Fujishima, A. Spin switching effect in nickel nitroprusside: design of a molecular spin device based on spin exchange interaction. *Chem. Mater.* **9,** 1092–1097 (1997).
115. Horie, M. *et al.* Thermally-induced phase transition of pseudorotaxane crystals: changes in conformation and interaction of the molecules and optical properties of the crystals. *J. Am. Chem. Soc.* **134,** 17932–17944 (2012).
116. Ye, H. Y., Zhang, Y., Fu, D. W. & Xiong, R. G. A displacive-type metal crown ether ferroelectric compound: $Ca(NO_3)_2$(15-crown-5). *Angew. Chem. Int. Ed.* **53,** 6724–6728 (2014).
117. Juhász, G. *et al.* Bistability of magnetization without spin-transition in a high-spin cobalt(II) complex due to angular momentum quenching. *J. Am. Chem. Soc.* **131,** 4560–4561 (2009).
118. De Panthou, F. L. *et al.* A new type of thermally induced spin transition associated with an equatorial ↔ axial conversion in a copper(II)–nitroxide cluster. *J. Am. Chem. Soc.* **117,** 11247–11253 (1995).
119. Hirel, C. *et al.* New spin-transition-like copper(II)-nitroxide species. *Inorg. Chem.* **46,** 7545–7552 (2007).
120. Fedin, M. *et al.* Light-induced excited spin state trapping in an exchange-coupled nitroxide-copper(II)-nitroxide cluster. *Angew. Chem. Int. Ed.* **47,** 6897–6899 (2008).
121. Barskaya, I. Y. *et al.* Photoswitching of a thermally unswitchable molecular magnet $Cu(hfac)_2L^{i\text{-}Pr}$ evidenced by steady-state and time-resolved electron paramagnetic resonance. *J. Am. Chem. Soc.* **136,** 10132–10138 (2014).
122. Tayi, A. S., Kaeser, A., Matsumoto, M., Aida, T. & Stupp, S. I. Supramolecular ferroelectrics. *Nature Chem.* **7,** 281–294 (2015).
123. Yannoni, C. S., Johnson, R. D., Meijer, G., Bethune, D. S. & Salem, J. R. ^{13}C NMR study of the C60 cluster in the solid state: molecular motion and carbon chemical shift anisotropy. *J. Phys. Chem.* **95,** 9–10 (1991).
124. Pekker, S. *et al.* Rotor–stator molecular crystals of fullerenes with cubane. *Nature Mater.* **4,** 764–767 (2005).
125. Das, D., Jacobs, T. & Barbour, L. J. Exceptionally large positive and negative anisotropic thermal expansion of an organic crystalline material. *Nature Mater.* **9,** 36–39 (2010).
126. Yao, Z. S. *et al.* Molecular motor-driven abrupt anisotropic shape change in a single crystal of a Ni complex. *Nature Chem.* **6,** 1079–1083 (2014).
127. Cai, H. L. *et al.* 4-(cyanomethyl)anilinium perchlorate: a new displacive-type molecular ferroelectric. *Phys. Rev. Lett.* **107,** 147601 (2011).
128. Fu, D. W. *et al.* 4-Methoxyanilinium perrhenate 18-Crown-6: a new ferroelectric with order originating in swinglike motion slowing down. *Phys. Rev. Lett.* **110,** 257601 (2013).
129. Akutagawa, T. *et al.* Ferroelectricity and polarity control in solid-state flip-flop supramolecular rotators. *Nature Mater.* **8,** 342–347 (2009).
130. Fu, D. W. *et al.* Diisopropylammonium bromide is a high-temperature molecular ferroelectric crystal. *Science* **339,** 425–428 (2013).
131. Tang, Y. *et al.* Hydrogen-bonded displacive-type ferroelastic phase transition in a new entangled supramolecular compound. *Cryst. Growth Des.* **15,** 457–464 (2015).
132. Sun, Z. *et al.* Ferroelastic phase transition and switchable dielectric behavior associated with ordering of molecular motion in a perovskite-like architectured supramolecular cocrystal. *J. Mater. Chem. C* **1,** 2561–2567 (2013).
133. Sorai, M. Entropy diagnosis for phase transitions occurring in functional materials. *Pure Appl. Chem.* **77,** 1331–1343 (2005).
134. Larionova, J. *et al.* Towards the ultimate size limit of the memory effect in spin-crossover solids. *Angew. Chem. Int. Ed.* **47,** 8236–8240 (2008).
135. Croce, R. & Van Amerongen, H. Natural strategies for photosynthetic light harvesting. *Nature Chem. Biol.* **10,** 492–501 (2014).
136. Coskun, A. *et al.* High hopes: can molecular electronics realise its potential? *Chem. Soc. Rev.* **41,** 4827–4859 (2012).

Acknowledgements

Support from MEXT (Japan); KAKEN (No. 15H01018, 26104528, 25288029) is gratefully acknowledged.

Additional information

Reprints and permissions information is available online at www.nature.com/reprints. Correspondence should be addressed to O.S.

Competing financial interests

The authors declare no competing financial interests.